Strain modeling of transpressional and transtensional deformation

HAAKON FOSSEN, BASIL TIKOFF & CHRISTIAN TEYSSIER

Fossen, H., Tikoff, B. & Teyssier, C. T.: Strain modeling of transpressional and transtensional deformation. *Norsk Geologisk Tidsskrift*, Vol. 74, pp. 134–145. Oslo 1994. ISSN 0029-196X.

Transpressional and transtensional deformation zones can be modeled as a simple shearing with a simultaneous component of pure shearing in the plane perpendicular to the zone. Four general types of deformation (pure shear- and wrench-dominated transpression/transtension) are distinguished on the basis of the instantaneous stretching axes. For each of these deformations the orientation of the finite strain ellipsoid, instantaneous stretching directions, flow apophyses, and rotation paths of lines and planes can be calculated. These quantities are reflected in the fabrics of deformed rocks (orientation and intensity of lineations, foliations, etc.) which can be used to qualitatively or quantitatively describe the deformation of both active and ancient transpressional/transtensional deformation zones. Partitioning of transpressional/transtensional displacement fields into pure shear-enhanced transpressional/transtensional domains separated by narrower strike-slip shear zones or faults can be modeled in the kinematic framework presented here, and may be applied to centimeter scale partitioning as well as to partitioning at the scale of plate boundary deformation zones.

H. Fossen, Statoil, GF/PETEK-GEO, N-5020 Bergen, Norway; B. Tikoff & C. Teyssier, Department of Geology and Geophysics, University of Minnesota, Minneapolis, MN 55455, USA

Steep deformation zones characterized by predominantly horizontal displacement have been documented in many tectonic settings in the Earth's crust during the last century and are commonly referred to as wrench or strike-slip zones (e.g. Wilcox et al. 1973; Sylvester 1988). These deformation zones are most commonly thought of as simple shear zones, but a closer evaluation reveals that simple shear is only one end member of more complex, three-dimensional deformation (e.g. Ramsay & Graham 1970; Tikoff & Fossen 1993; Simpson & De Paor 1993). Because of vertical or lateral irregularities, external boundary conditions, or changing kinematics, these zones usually deviate from simple shear.

A full spectrum of deformations exists between simple shear strike-slip deformation and plane-strain extension, as well as between simple shear strike-slip deformation and plane-strain contraction. These two spectra are called transtensional and transpressional deformations, respectively (Fig. 1) (also referred to as divergent/convergent strike-slip zones), and have been receiving increasing attention during the last decade or so (e.g. Wilcox et al. 1973; Sanderson & Marchini 1984; Harding 1985; McCross 1986; Ratschbacher 1986; Hudleston et al. 1988; Sylvester 1988; Oldow 1990; Bürgman 1991; Fossen & Tikoff 1993).

The fact that many zones of horizontal displacement involve some shortening or extension across them has important local or regional implications for three-dimensional strain, and therefore calls for a closer examination of these phenomena. A major challenge is to obtain knowledge about transpression/transtension so that one can distinguish between different types of these deformations and, if possible, quantify the deviation from simple shear. As a prerequisite, the characteristics of the various deformation types must first be known and understood.

There are at least three approaches to this problem. One is detailed mapping of non-simple shear strike-slip zones where the boundary conditions are known from independent sources. Although some field criteria have been developed for this type of study (e.g. Simpson & De Paor 1993), suitable field examples may, however, be hard to find. Hence, some workers have attempted to simulate this type of deformation with physical modeling which allows a good control of boundary conditions. Although experiments of this type tend to be difficult and time-consuming, useful results have been obtained (e.g. Wilcox et al. 1973; Withjack and Jamison 1986; Tron & Brun 1991).

Another possible approach is explored in this work, i.e. numerical modeling of transpressional/transtensional deformation. Although there is a limit to the complexities that can be incorporated in numerical simulations, the boundary conditions are precisely known, and exact solutions concerning parameters, such as finite and incremental strain and rotation of strain markers, may be calculated as a function of deformation.

In this article we explore the full spectrum of deformations represented in Fig. 1 with emphasis on the implications for ductile and brittle deformation of the crust.

The model

A simple and useful model was suggested by Sanderson & Marchini (1984) for transpression (Fig. 2), where a vertical strike-slip zone that is undergoing simple shearing

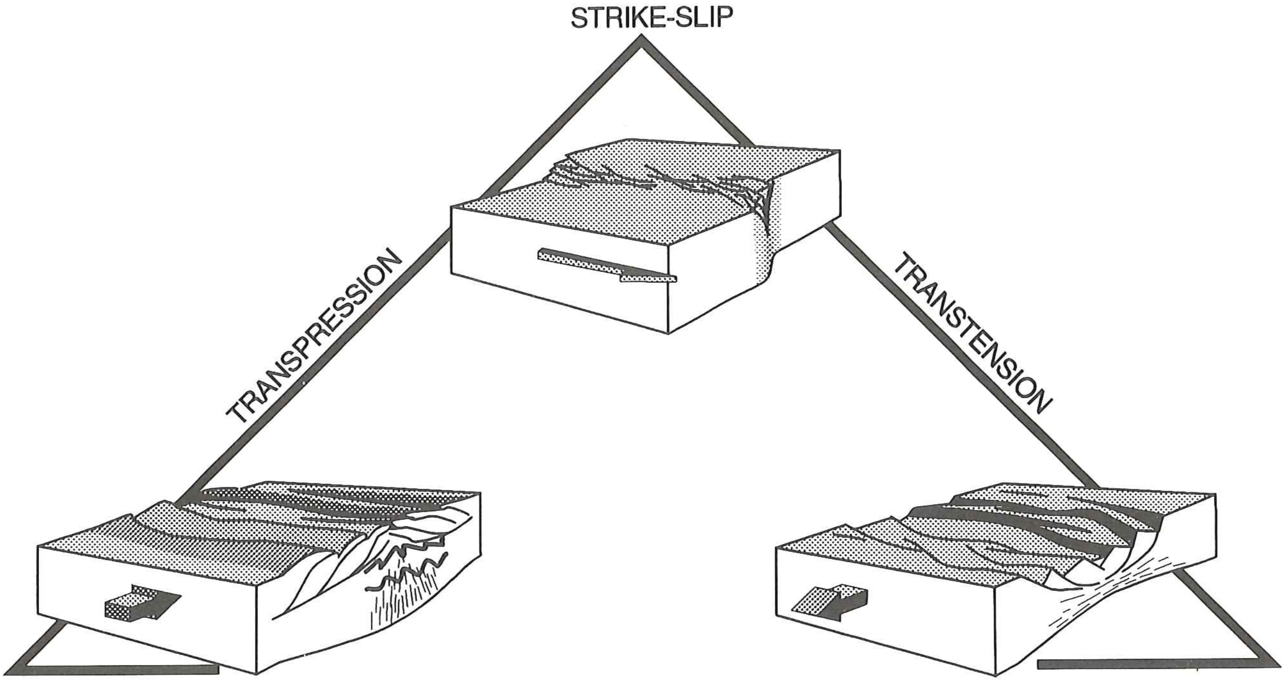

Fig. 1. Illustration of three end members of simple crustal deformation: strike-slip (vertical simple shear), plane strain contractional and plane strain extensional deformation.

is simultaneously affected by a component of horizontal shortening perpendicular to the shear zone. The horizontal shortening (or extension in transtension) is perfectly compensated by a vertical extension (shortening) so that volume is preserved. Hence, we are concerned with a simultaneous simple and pure shearing deformation which can be described by the following deformation matrix (position gradient tensor):

$$\mathbf{D} = \begin{bmatrix} 1 & \Gamma & 0 \\ 0 & k & 0 \\ 0 & 0 & k^{-1} \end{bmatrix} = \begin{bmatrix} 1 & \dfrac{\gamma(1-k)}{\ln(k^{-1})} & 0 \\ 0 & k & 0 \\ 0 & 0 & k^{-1} \end{bmatrix}. \quad (1)$$

Any point or vector $\mathbf{x}$ before deformation is transformed to a new position $\mathbf{x}'$ after deformation by the linear transformation

$$\mathbf{x}' = \mathbf{D}\mathbf{x} \quad (2)$$

(see Fossen & Tikoff 1993). The matrix $\mathbf{D}$ describes a homogeneous deformation, where γ is the shear strain from the simple shear component, and k is the factor by which the zone is shortened/extended (for example, $k = 0.7$ implies 30% shortening across a transpressional deformation zone; if $k = 1$ there is no shortening and if $k = 1.2$ there is 20% extension across a transtensional deformation zone). Once the matrix $\mathbf{D}$ is formed, the exact orientation and magnitude of the finite or incremental strain ellipsoid can easily be calculated (see Fossen & Tikoff 1993). Furthermore, the orientation of passive linear and planar markers after deformation can be studied. The deformation history, e.g. the rotation paths of linear structures or the temporal development of the strain ellipse can also be found by successively applying an incremental deformation matrix $\mathbf{D}$.

In the following section, we explore transpression and transtension by considering a vertical shear zone oriented in a Cartesian coordinate system such that the x-axis is parallel to the horizontal simple shear displacement direction, y is horizontal and perpendicular to the shear zone, and z is vertical (Fig. 2).

Instantaneous stretching directions and the four classes of transpression/transtension

The instantaneous stretching axes (also commonly denoted as the maximum, intermediate, and minimum strain rates or axes of the instantaneous strain ellipse) are of particular interest because they influence the accumulating deformation and deformation structures, and they can in some cases be extracted from deformed rocks from studying fiber growth, vein sets, etc. (cf. Elliott 1972; Ramsay & Huber 1983). Furthermore, under certain restricted conditions the instantaneous stretching axes may be equated to principal stresses (cf. Weijermars 1991).

In our model, one of the instantaneous stretching axes is always vertical (parallel to z), whereas the other two are in the horizontal ($x-y$) plane. It is interesting to note how the orientation of the instantaneous stretching axes is directly related to the kinematic vorticity number (Wk)

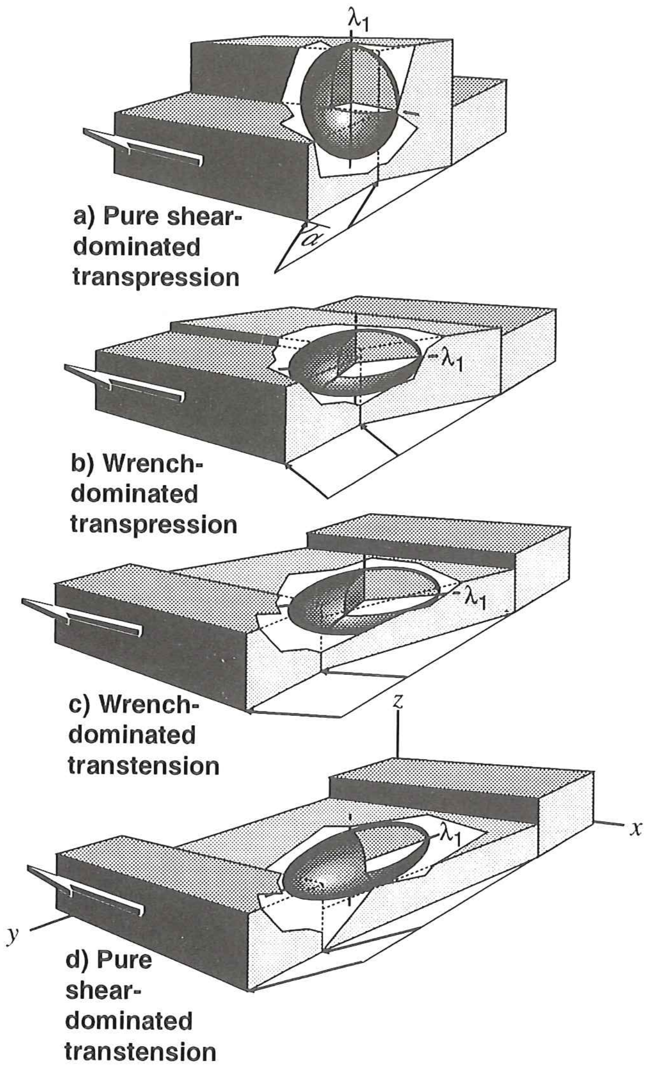

Fig. 2. The four classes of transpression/transtension that emerge from the model suggested by Sanderson & Marchini (1984). The finite strain ellipses are shown in each case.

of the deformation (Truesdell 1953). *Wk* is a measure of the coaxiality of progressive deformation, and has the value of 1 for simple shearing and 0 for pure shearing (Means et al. 1980). If $Wk = 1$ (simple shear wrenching), then no stretching occurs in the vertical direction, and the maximum and minimum instantaneous stretching axes are oriented exactly 45° to the shear zone. If there is a small component of pure shear acting simultaneously with the simple shearing ($Wk > 0.81$), the intermediate instantaneous stretching axis will still be vertical, but the angle between the maximum instantaneous stretching axis and the shear zone will be lower (for transpression) or higher (for transtension) than 45°. However, there is a fundamental difference for deformations with $Wk < 0.81$, in which case the largest instantaneous stretching axis is vertical if deformation is transpressional. In transtension, the smallest instantaneous stretching axis (i.e. the maximum instantaneous contraction direction) is vertical if $Wk < 0.81$ (Table 1). This suggests a subdivision of transpression and transtension into four different classes: (1) *wrench-dominated transpression* ($1 > Wk > 0.81$), which includes simple shearing with a weak to moderate component of simultaneous pure shearing causing the horizontal maximum instantaneous stretching axis to be oriented 45–35° to the shear zone (Fig. 3a); (2) *wrench-dominated transtension* ($1 > Wk > 0.81$), where the horizontal maximum instantaneous stretching axis makes 45–55° to the shear zone; (3) *pure shear-dominated transpression* ($Wk < 0.81$), where the maximum instantaneous stretching axis is vertical, and (4) *pure shear-dominated transtension* ($Wk < 0.81$), where the minimum instantaneous stretching axis is vertical.

The orientation of the instantaneous stretching axes has implications for the initial orientation of folds. Although the initiation of folds is not completely understood, it is a common assumption that folds initiate with axes perpendicular to the maximum instantaneous shortening direction in the plane of the layering. If the layering is horizontal, as in a sedimentary basin, the fold axes are expected to form parallel to the largest instantaneous stretching axis in the horizontal plane (Treagus & Treagus 1981). This implies that, for the case of horizontal layering, fold axes initially make an angle of θ with the deformation zone, where θ (the angle between the shear zone boundary and the maximum

Table 1. Some important characteristics for the different types of deformation covered by Fig. 1. See also Fig. 2.

		TRANSPRESSION				TRANSTENSION			
	PURE SHEAR (CONTRACTION)	PURE SHEAR-DOMINATED		WRENCH-DOMINATED	SIMPLE SHEAR	PURE SHEAR-DOMINATED		WRENCH-DOMINATED	PURE SHEAR (EXTENSION)
	$W_k=0$	$0<W_k<0.81$	$W_k=0.81$	$0.81<W_k<1$	$W_k=1$	$1>W_k>0.81$	$W_k=0.81$	$0.81>W_k>0$	$W_k=0$
Fabric	LS	(L)S	S	(L)S	LS	L(S)	L	L(S)	LS
Stretching lineation	vertical	vertical	none → weak vertical	horizontal, oblique → vertical	horizontal, oblique to shear zone	horizontal, oblique to shear zone	horizontal, oblique to shear zone	horizontal, oblique to shear zone	horizontal, perpend. to shear zone
Foliation	vertical, parallel to shear zone	vertical, oblique to shear zone	vertical, oblique to shear zone	vertical, oblique to shear zone	vertical, oblique to shear zone	vertical, oblique → horizontal	none → week horiz.	horizontal	horizontal
Strain	plane strain	general flattening	perfect → general flattening	general → perfect → gen. flattening	plane strain	gen. → perfect → gen. constrict.	perf. → gen. constriction	general constriction	plane strain
Max. inst. stretching axis	vertical	vertical	spans vertical plane inclined 35° to shear zone	horizontal, 35-45° to shear zone	horizontal, 45° to shear zone	horizontal, 45-55° to shear zone	horizontal, 55° to shear zone	horizontal, 55-90° to shear zone	horizontal, 90° to shear zone

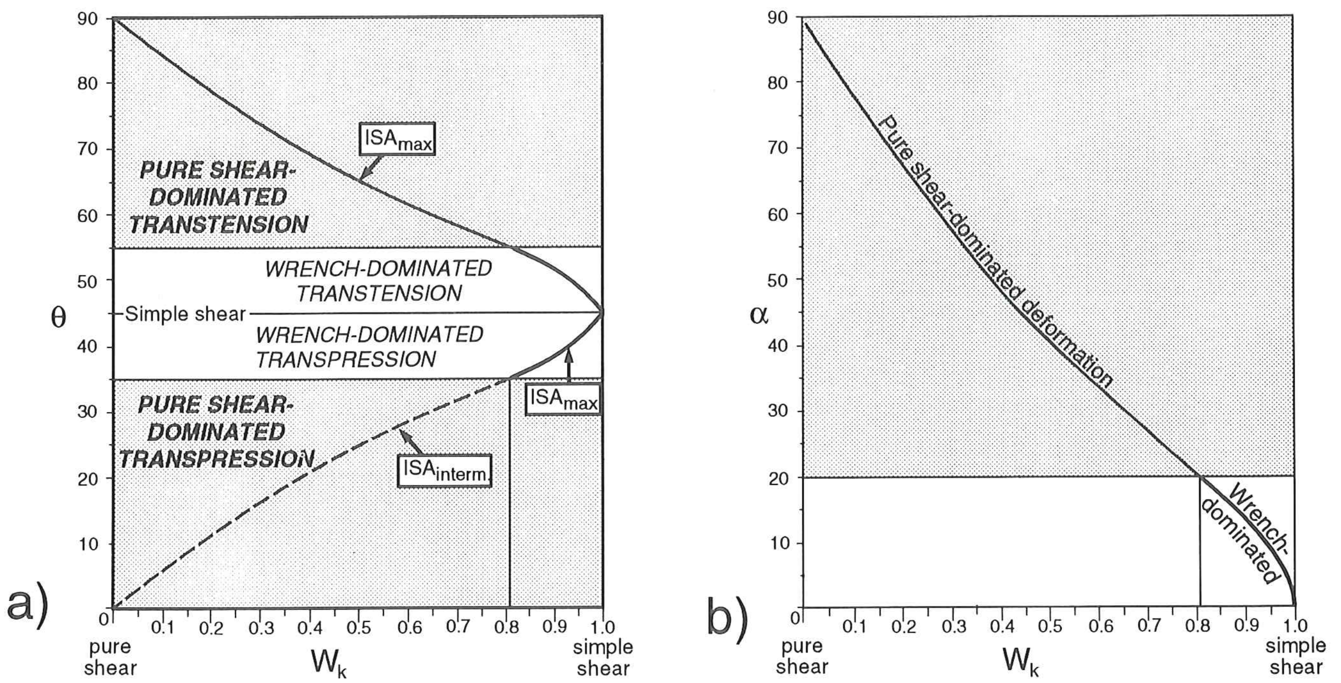

Fig. 3. (a) Angle θ between the maximum horizontal instantaneous stretching axis (ISA) and the deformation zone boundary as a function of the kinematic vorticity number Wk. Note that the maximum ISA is vertical for pure shear-dominated transpression, and thus the intermediate ISA is the largest ISA in the horizontal plane. (b) The relationship between α (acute angle between the oblique, horizontal flow apophysis and the deformation zone boundary) and Wk. Because of the way (a) is defined, this graph covers both transpression and transtension.

instantaneous stretching direction in the horizontal plane) can be found from Fig. 3a.

Flow apophyses

Flow apophyses characterize the flow of particles (stream lines) at any instant, and are useful to consider in the modeling of deformation (Bobyarchick 1986; Passchier 1990). They are the axes of maximum, intermediate and minimum gradient of particle movement, and define a unique set of straight particle paths with orientations that depend on the type of deformation. No particles can cross any of the flow apophyses during deformation, and the flow apophyses may be considered as defining starting and ending points of rotating lines and poles to planes during deformation (see below).

For our model of transpression/transtension, one flow apophysis is always vertical, one is parallel to the x-axis, and one lies in the horizontal $x-y$ plane and is generally oblique to the x-axis (Fig. 3b). The angle between the oblique flow apophysis and the shear zone varies from 0 to 90° in the $x-y$ plane, depending on Wk or the relative amount of pure shearing (leading to area change in the $x-y$ plane) and simple shearing. The angle α that the oblique flow apophysis makes with the shear zone is

$$\alpha = \tan^{-1}[(\ln k)/\gamma]. \qquad (3)$$

Note that α is different from the angle θ between the maximum stretching direction and the shear zone (Fig. 3a, b). The flow pattern in the plane containing the oblique flow apophysis and the z-axis (a vertical plane) is that of pure shear (Fig. 4b). The $x-z$ vertical plane also contains two flow apophyses; the flow is shown in Fig. 4c.

In this work, we assume that steady-state deformation, i.e. that the orientation of the flow apophyses (α) and the instantaneous stretching axes (θ), remains constant relative to the shear zone during deformation.

Rotation of passive markers

Linear or planar markers in transpressional/transtensional deformation zones rotate during progressive deformation according to the relative contribution of simple and pure shear components (e.g. Passchier 1990). Such markers include pre-existing features; bedding, current directions, dikes, earlier fold axes and intersection lineations, or igneous or metamorphic (linear and planar) fabrics. Structures that form during deformation (folds, intersection lineations, etc.), alre also affected by subsequent deformation.

Rotation of passive linear markers

Linear markers rotate along paths that depend on the kinematic vorticity number of the deformation (Fig. 5). For simple shear wrenching, passive lines move along great circles (Fig. 5, top), whereas for pure shearing ($Wk = 0$), the rotation pattern is symmetric about the three orthogonal flow apophyses (orthorhombic symmetry).

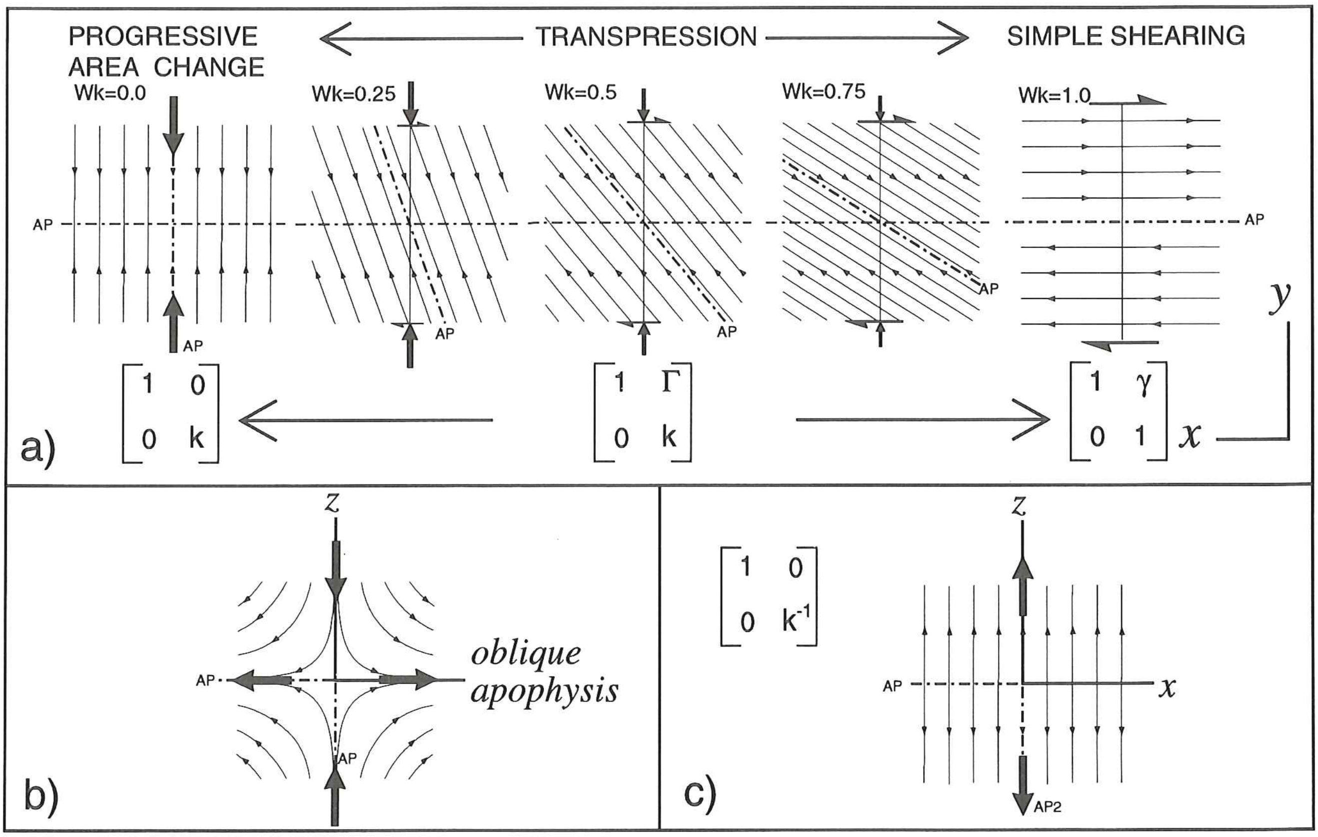

Fig. 4. Particle paths and flow apophyses (AP's) (a) in the xy (horizontal) plane for various kinematic vorticity numbers in transpression, (b) in the vertical plane that contains the oblique flow apophyses (AP-z plane, which is a plane of pure shear), and (c) in the vertical x–z plane (deformation is area change in this section). The sectional deformation matrix is indicated for (a) and (c).

For transtension, the flow pattern is governed by the oblique, horizontal flow apophysis. With the accumulation of high strain, any line (except perfectly vertical ones) will tend to become parallel to the *oblique* flow apophysis. This is an important observation, since it means that rotated linear features in transtensional zones should be concentrated about a horizontal direction which is oblique to the shear zone. If the angle between linear elements and the shear zone can be constrained, the angle α between the flow apophyses and the shear zone can be approximated, and hence the average kinematic vorticity number of the deformation can be determined (Fig. 3b).

In the case of transpression, passive line markers rotate along paths that start at the oblique flow apophysis, and rotate towards a vertical position as finite strain increases. Hence, high-strain transpressional zones would tend to have vertical lineations, even in the case of wrench-dominated transpression.

In addition to defining the theoretical rotation paths, it is useful to study the deformation of a certain distribution of linear markers. Fig. 6 shows the effect of deforming 500 randomly oriented passive line markers for two cases of transtensional deformation ($Wk = 0.5$ and 0.85). As predicted from the theory and Fig. 5, the lines end up parallel to the oblique flow apophysis. After a deformation of $\bar{\varepsilon}_s = 2$, which corresponds to $\gamma = 3.524$ and $k = 1.454$ for $Wk = 0.85$, and $\gamma = 2.793$ and $k = 2.376$ for $Wk = 0.85$, a high concentration of lines is achieved ($\bar{\varepsilon}_s = (\sqrt{3}/2)\gamma_0$ where γ_0 is the natural octahedral strain; see Hossack 1968). It is important to note that, due to the asymmetric rotation paths illustrated in Fig. 5, the maximum that forms early during deformation is *not* parallel to the oblique flow apophyses, but the difference decreases as strain increases.

The obliquity between the maximum and the flow apophysis is more pronounced in the case of wrench-dominated transtension because of the greater non-coaxial component of deformation (Fig. 6). The actual orientation of passively deformed linear features in a specific transpression/transtension zone depends on the initial orientation of the markers, the strain intensity, and the nature of the deformation. If we know the orientation of a pre-existing set of linear features outside the shear zone, and can make two or more observations of their orientations at different states of strain within the zone, the orientations can be plotted on diagrams like Fig. 5. From this it is possible to determine whether the zone is transpressional, simple shear, or transtensional, and in some cases the average kinematic vorticity number of the deformation can be estimated.

Rotation of planar markers

Passive planar markers can be traced during deformation, similar to the rotation of line markers. As for lines,

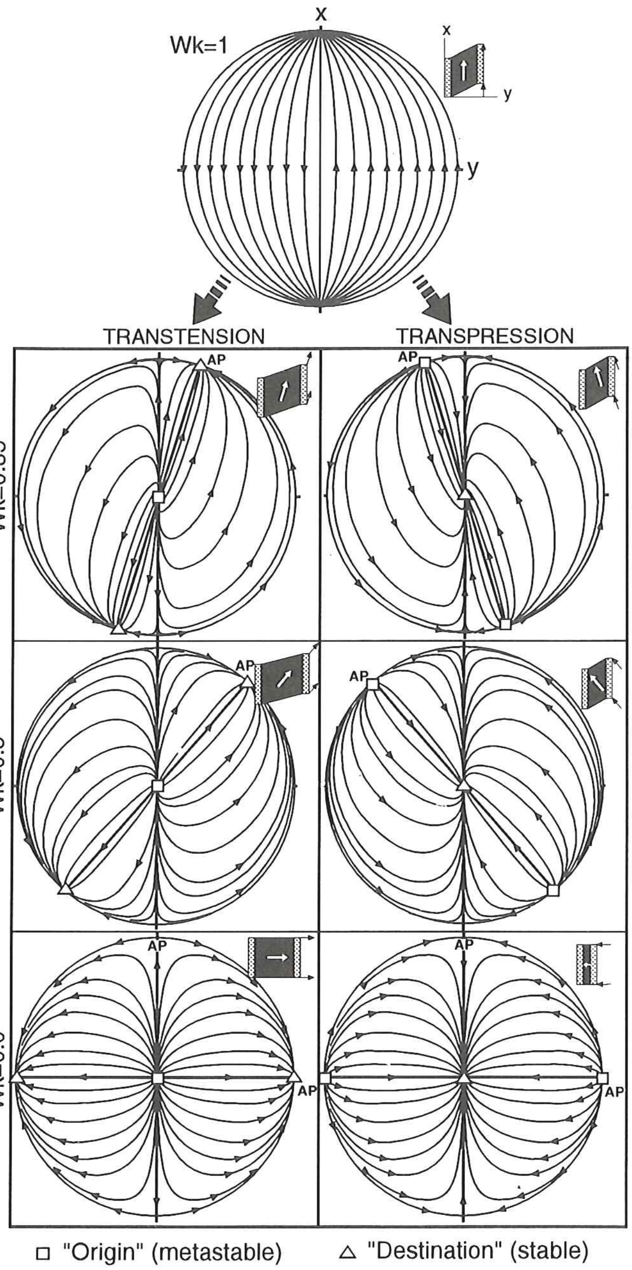

Fig. 5. Rotation paths of passively deforming lines for sinistral simple shear wrenching (top, $Wk = 1$) and various cases of transpression, transtension, and pure shear (bottom, $Wk = 0$). For cases where $0 < Wk < 1$, i.e., transpression or transtension, the oblique straight path is parallel to the oblique flow apophyses, and its orientation is therefore determined by eq. 3. Small deformation boxes contain the flow apophyses (white) that determine the stable position of passively deforming lines.

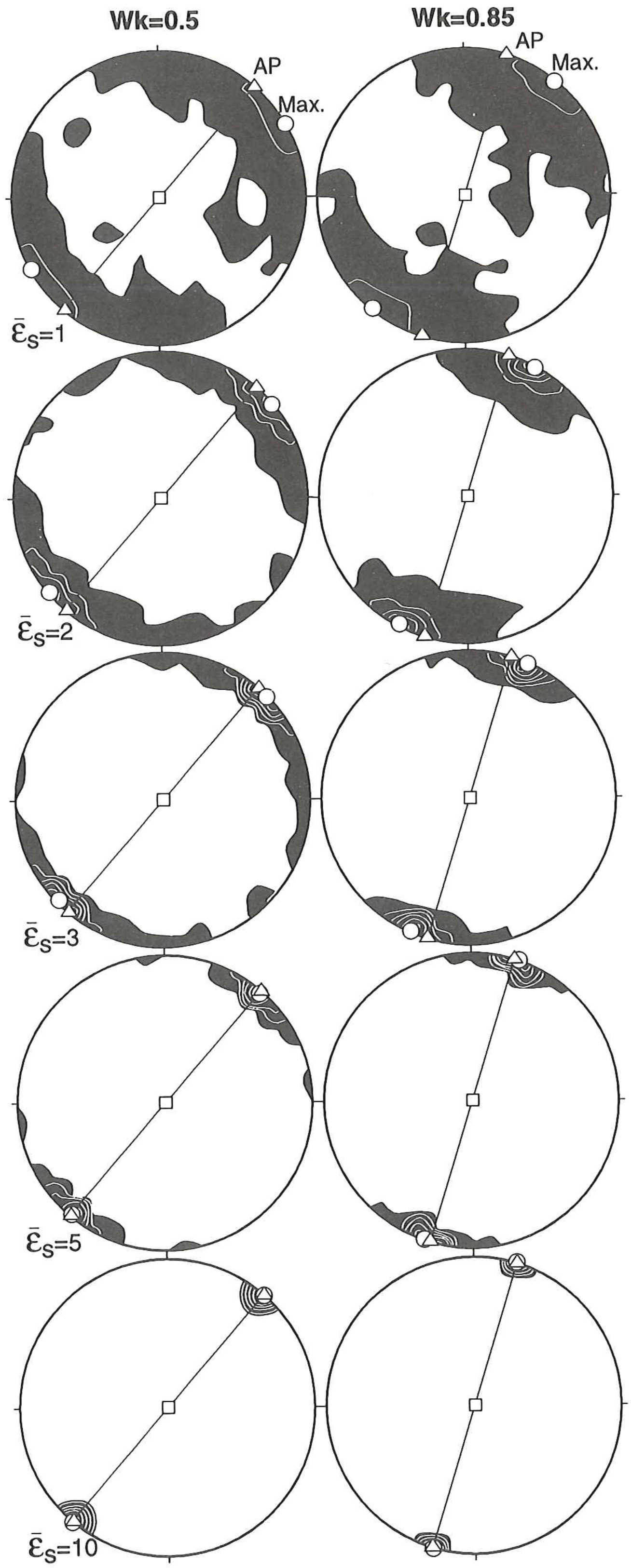

Fig. 6. The result of progressive passive deformation of 500 randomly oriented lines for a case of pure shear-dominated transtension ($Wk = 0.5$) and wrench-dominated transtension ($Wk = 0.85$). Contoured by the Kamb method at 1, 10, 30, 50, and 70% intervals ($\sigma = 2$). See text for discussion.

the rotation paths (Fig. 7) are largely controlled by the flow apophyses which again are directly dependent on *Wk*. In simple shear (Fig. 7, top) the poles to planes move along great circles so that all planes (except those that strike perfectly parallel to x) rotate towards a vertical position as the shear strain approaches infinity.

Transtensional deformation results in rotation of planes towards a horizontal position. The rotation path of poles to planes is towards the oblique flow apophysis and subsequently towards the center of the stereo net (Fig. 7). This contrasts strongly with the case of transpression, where passively deformed planes end up vertical, parallel to the deformation zone boundary. Hence,

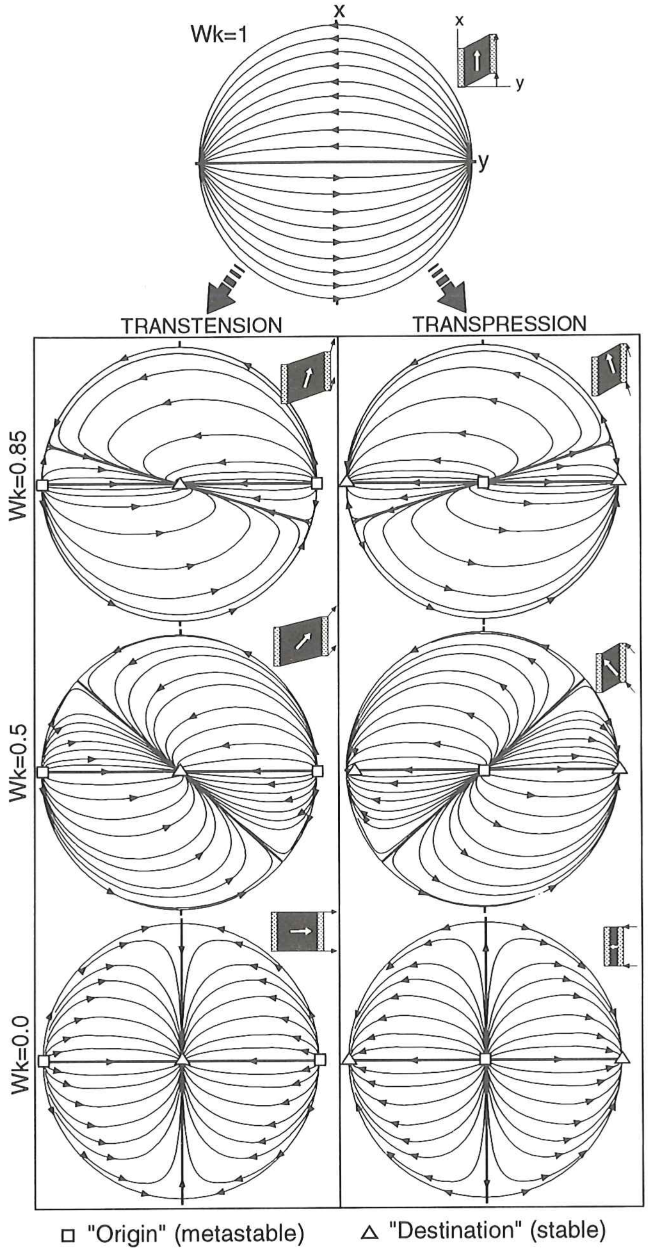

Fig. 7. Rotation paths of passively deforming poles to planes for the same deformations as in Fig. 5. The acute angle between the two straight paths equals the angle between the two horizontal flow apophyses, and may be determined by eq. 3. See also Fig. 5.

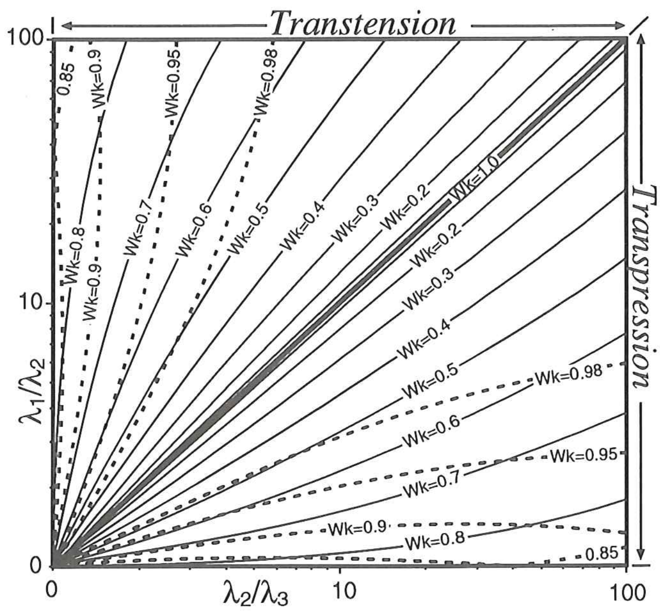

Fig. 8. Constant *Wk* paths shown in a logarithmic Flinn diagram. Dashed lines indicate wrench-dominated transtension/transpression, and solid lines are pure shear-dominated deformations. Wrench-dominated paths eventually hit the coordinate axes (see path for $Wk = 0.85$), and two of the finite strain axes then switch positions.

transpressional/transtensional shear zones can be distinguished by the orientation of deformed planar markers in the deformation zone.

Finite and incremental strain

The shape of the finite strain ellipse is always oblate (flattening strain) for transpression, and prolate (constrictional strain) for transtension (Sanderson & Marchini 1984). Modeling the development of the finite strain ellipsoids for steady-state (constant *Wk*) deformations shows that even a very weak component of pure shear in a wrench-dominated deformation leads to strain ellipsoids far into the flattening/constrictional field (Fig. 8). Pure flattening/constriction (the abscissa and ordinate axes of the Flinn diagram, Fig. 8) is only found instantaneously for steady-state deformations with $1 > Wk > 0.81$. At the limit between wrench-dominated and pure shear-dominated deformation, i.e. at $Wk = 0.81$, the instantaneous strain ellipsoid is one of pure flattening, but eventually the pure shear component becomes dominant and the finite strain is increasingly plane strain. The consequence is that any given finite strain geometry may be the result of either a wrench-dominated or a pure shear-dominated deformation. This is a generalization of the well-known fact that strain ellipsoids resulting from pure and simple shearing are inseparable by shape alone, since the paths of $Wk = 1$ and $Wk = 0$ coincide in Flinn space (both have a Flinn k-value of 1). Because there is more than one kinematic vorticity number associated with each point in the Flinn space, the two cases (pure shear- and wrench-dominated deformations) must be distinguished by some other means. For example, if an incremental strain can be recognized, one may be able to separate between the two different paths. More commonly, the *orientation* of the horizontal strain ellipse can be determined in the field, and Fig. 9 can be used to determine the type of deformation. If the maximum finite stretching direction is known, Figs. 2 and 10 may be used.

The maximum horizontal strain axis (λ) makes an angle θ' with the deformation zone boundary:

$$\theta' = \tan^{-1}[(\lambda - \Gamma^2 - 1)/k\Gamma]. \qquad (4)$$

Knowing the aspect ratio R for the horizontal strain ellipse and its orientation θ', one can estimate *Wk* by using Fig. 9.

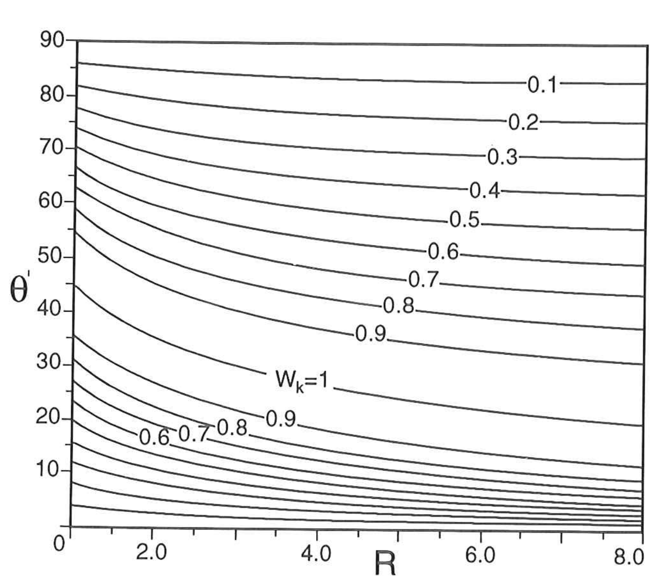

Fig. 9. Relationship between R (aspect ratio of the two horizontal principal strains) and the angle between the largest horizontal principal strain and the transpressional/transtensional deformation zone in terms of the kinematic vorticity number *Wk*. Assuming steady-state deformation, this graph can be used to estimate *Wk* for a transpressional/transtensional deformation.

The progressive development of the strain ellipse is fundamentally different for pure shear and simple shear-dominated deformations (Fig. 10). For pure shear-dominated transpression, λ_1 is always vertical, and for pure shear-dominated transtension, λ_3 remains vertical throughout deformation. However, for wrench-dominated transpression and transtension, λ_2 starts out as the vertical principal strain axis, but switches position with λ_1 (transpression) or λ_3 (transtension) at some point during deformation. During a progressive deformation, this change happens earlier the closer *Wk* is to 0.81, and

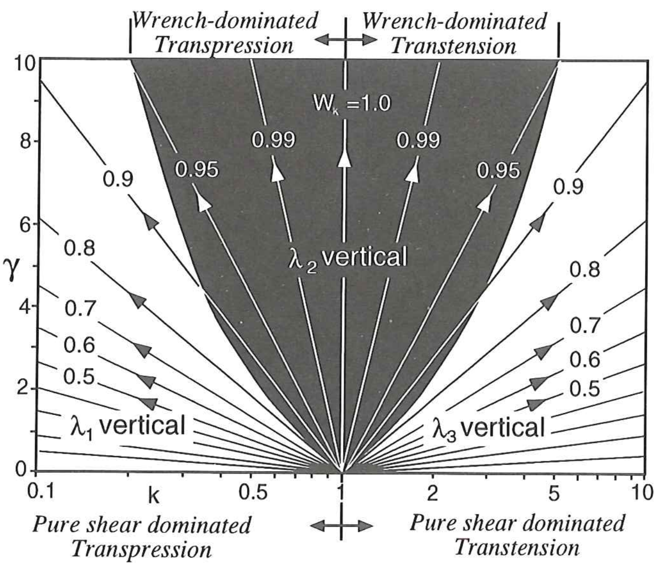

Fig. 10. Areas of various finite strain orientations in terms of the pure shear (k) and simple shear (γ) components of transpression/transtension (see eq. 1). These areas define the fields of wrench (simple shear) and pure shear-enhanced deformations. Note that constant *Wk* paths are straight lines when k (horizontal axis) is plotted logarithmically. Modified from Fossen & Tikoff (1993).

for deformations close to simple shear ($Wk = 1$) the switch occurs at such high strains that it is unlikely to be recorded in naturally deformed rocks. Similarly, λ_2 and λ_3 switch positions during wrench-dominated transtension. It may be noted that this switch of finite strain axes occurs as the deformation path coincides with one of the axes in the Flinn diagram (Fig. 8).

The evolution of finite strain has important consequences for the development of fabrics in rocks (Table 1). Stretching lineations are closely related to the finite strain ellipsoid, provided that the viscosity contrast between the deforming object and the matrix is low. Hence, we can predict that L-fabrics and horizontal stretching lineations are best developed in pure-shear or wrench-dominated transtensional deformations. LS fabrics are typical of wrench-dominated transpressional deformations where the stretching lineation is horizontal. However, with an increasing pure shear component and/or high strain, wrench-dominated transpression leads to strong flattening (S) fabrics, and thus the associated vertical stretching lineations are weakened. The planar fabric produced during such deformations is also vertical and oblique to the shear zone. Finally, pure shear-dominated transpression gives rise to (L)S fabrics with vertical, oblique foliations and vertical lineations.

Strain partitioning and application to orogenic deformation

The model outlined above is one of homogeneous deformation, which is a simplified condition restricted to a scale typically smaller than that of the width of a deformation zone. To model the entire deformation system, one may obtain a sufficient degree of accuracy by subdividing the system into a number of domains, each of which is treated as a domain of homogeneous deformation. Heterogeneous deformation can also be modeled directly by replacing constants of the deformation matrix with functions. For the case of transpression/transtension, a reasonable model may be to assume an evenly distributed shortening/extension across the deformation zone, and a simple shear component that increases towards the center of the zone. This can be modeled by the deformation matrix

$$\mathbf{D} = \begin{bmatrix} 1 & \dfrac{f(y)(1-k)}{\ln(k^{-1})} & 0 \\ 0 & k & 0 \\ 0 & 0 & k^{-1} \end{bmatrix} \qquad (5)$$

where $f(y)$ is the shear strain (γ) as a function of y, varying from 0 at the margin of the deformation zone to some maximum value in the middle of the zone. Such γ-functions tend to be non-linear, and have been graphically presented by various authors for cases where $Wk \approx 1$ by methods outlined in Ramsay & Huber (1983) (e.g. Simpson 1983).

In other cases it may not be appropriate to consider deformation as gradually changing from the margins to the core of deformation zones, since changes may be very abrupt and localized. This common phenomenon is referred to as strain partitioning, and occurs from the centimeter scale (e.g. Bell 1981; Lister & Williams 1983; Law et al. 1984; Dennis & Secor 1990) up to the scale of several tens of kilometers, e.g. along plate boundaries (Fitch 1972; Mount & Suppe 1992; Pinet & Cobbold 1992; Jackson 1992). In any of these cases it may be useful to consider the deformation as homogeneous within the different zones or domains of similar deformation type.

The simplest and probably most common form of strain partitioning in transpression/transtension is the case where domains of wrench-dominated and pure shear-enhanced (generally pure shear-dominated) deformation alternate, and where each domain is characterized by its own orientation and geometry of the finite strain ellipsoid, orientation of the instantaneous stretching directions, rotation pattern of passive markers, and preferred orientations of deformed lines and planes. In such cases, the pure shear-enhanced zones tend to be wide, whereas the wrench-dominated zones are narrower and may be represented by either a narrow, ductile shear zone (Fig. 11b) or a fault or fault zone (Fig. 11a). It is possible to recognize and describe such strain partitioning in the field using the criteria outlined in this paper (Table 1). For instance, in transpressional deformation zones one may expect pure shear-dominated domains where the foliation is vertical and almost parallel to the deformation zone, the stretching lineation is vertical but poorly developed, and the finite strain is of the flattening type, separated by narrower zones of vertical foliation and horizontal stretching lineation oblique to the deformation zone where the finite strain is closer to plane strain.

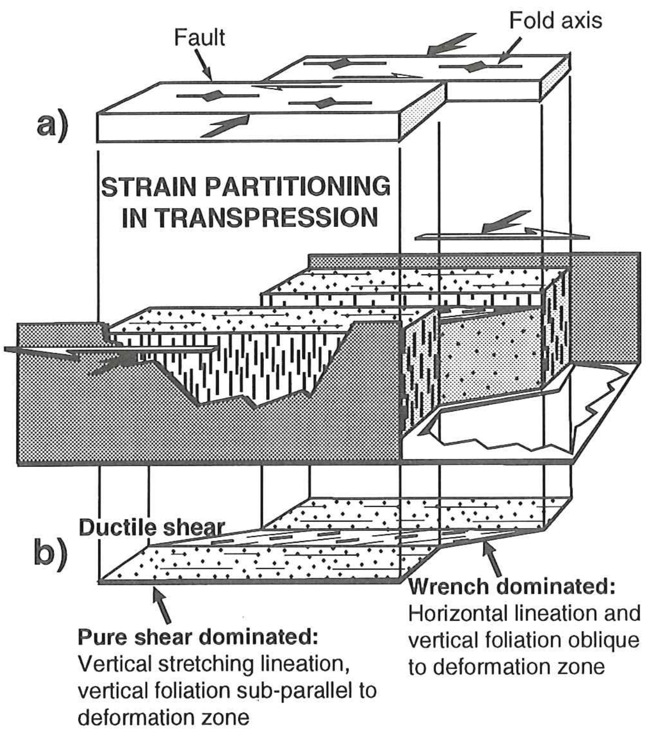

Fig. 11. Illustration of strain partitioning in a transpressional deformation zone. (a) Partitioning in the brittle-ductile regime, where the shear component is accommodated by a vertical fault and the adjacent areas are dominated by pure shear. (b) Partitioning in the ductile regime with the development of different fabrics in the simple shear and pure shear-dominated zones.

Transpression/transtension cover an important range of crustal deformations associated with orogenic belts or plate margins (Fig. 1). Plate movements are generally oblique to plate boundaries (e.g. DeMets et al. 1990), i.e. both divergent and convergent plate boundaries are likely to experience a component of margin-parallel movement. As proposed by a number of authors (e.g. Fitch 1972; Walcott 1984; Woodcock 1986; Mount & Suppe 1987; Zoback et al. 1987; Oldow et al. 1989; McCaffrey 1991; Vauchez & Nicholas 1991; Cashman et al. 1992; Diament et al. 1992; Jackson 1992; Mount & Suppe 1992; Pinet & Cobbold 1992), the deformation along both ancient and modern plate boundaries is partitioned in various ways, particularly by zones of lateral shear and domains of horizontal contraction. This type of partitioning may be applied to explain present and ancient convergent plate margins where strike-slip movement coexists or coexisted with orogen-normal deformation, such as the Himalayan collision zone and the Alps (e.g. Tapponnier et al. 1986; Laubscher 1971; Hubbard & Mancktelow 1992). It is possible to apply our model to these large-scale settings since the flow apophyses are directions of maximum displacement gradient, and therefore one flow apophysis is parallel to the relative plate motion vector. The angle α between the contractional flow apophysis and the deformation zone in transpression equals the angle between the relative plate motion direction and the plate boundary (McKenzie & Jackson 1983; Tikoff & Teyssier 1994). This very important observation allows us to model the effect of various types of convergent or divergent plate boundaries, with the plate motion vector and the orientation and degree of strain partitioning of the deformation zone as variables. Thus, the total *Wk* of the plate boundary deformation zone can be found from the orientation of the plate motion vector (α) by using the graph in Fig. 3b.

If the deformation is partitioned between contractional (pure shear enhanced) domains and narrow simple shear (fault) zones parallel to the plate boundary, then, for a given plate motion, the amount of displacement along discrete faults or narrow shear zones determines the relative amount of pure and simple shear (*Wk*) in the contractional domains. The higher the cumulative displacement along faults, the closer to pure shear is the deformation between the faults and vice versa (Fig. 12). This has been explored for some present-day convergent plate boundaries (Tikoff & Teyssier 1994), such as the San Andreas fault system, where the plate vector makes an angle (α) of approximately 5° with the plate boundary (Zoback & Zoback 1991) (Fig. 13). Using Fig. 3a and b,

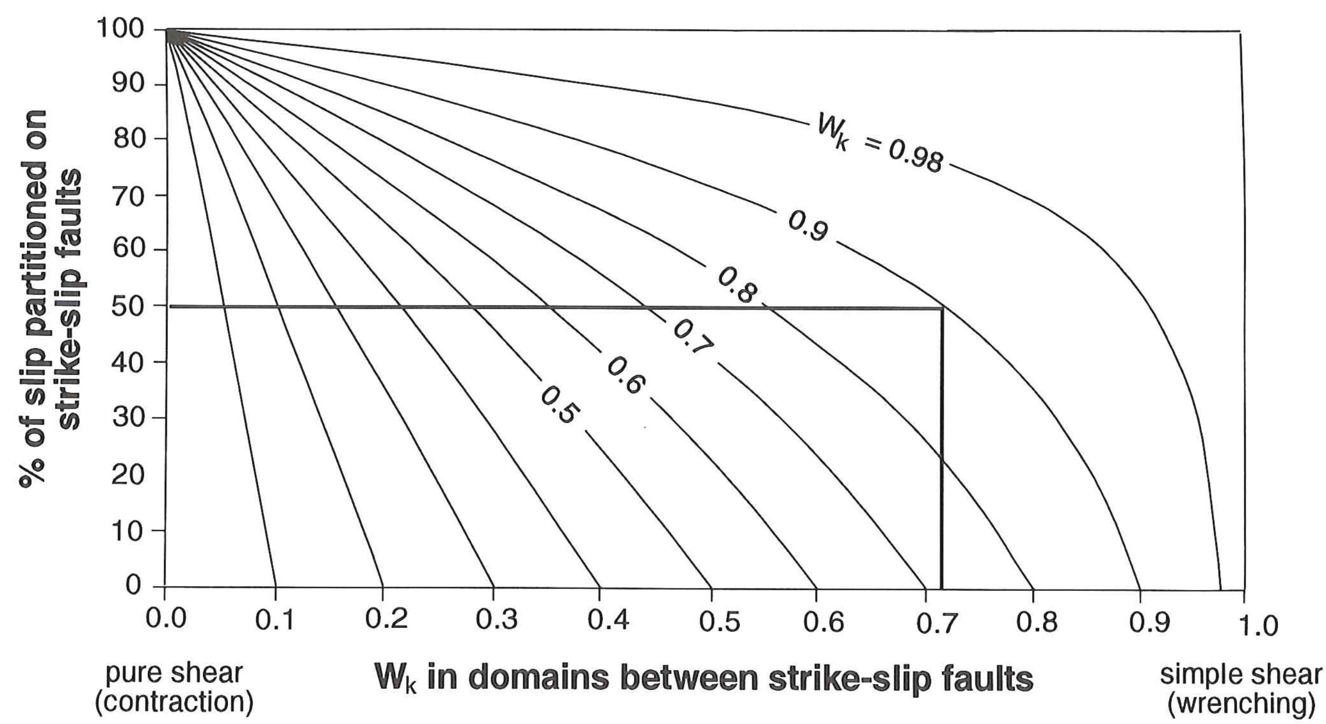

Fig. 12. Relationship between *Wk* within the pure shear-enhanced domains between discrete strike-slip faults (horizontal axis) and % of shear displacement absorbed by faults for a transpressional zone (vertical axis). Contours of *Wk* for the deformation zone as a whole (from boundary conditions, e.g. plate motions) show how increased slip partitioning results in an increased pure shear component in the domains between the faults. For instance, a transpression zone where the boundary conditions impose a *Wk* of 0.9 on the zone (i.e. wrench-dominated transpression) results in domains with $Wk = 0.72$ (pure-shear dominated transpression) if 50% of the slip is taken up along discrete faults. If 100% of the slip is accommodated by faults parallel to the plate boundary, the deformation between the faults is always a perfect pure shear ($Wk = 0$) regardless of the overall or 'average' *Wk* for the deformation zone, and no partitioning implies that *Wk* is spatially constant within the zone.

this indicates that the contractional instantaneous stretching axis is oriented at 42.5° to the plate margin and $Wk \approx 0.985$ for the total deformation zone (i.e. wrench-dominated deformation close to simple shear). However, because a very significant amount of lateral simple shear (more than 95%) is taken up along the fault system, domains between the faults must accommodate the remaining pure shear or convergent component of the plate motion, and thus must experience pure shear-dominated transpression. This implies that the largest horizontal instantaneous stretching direction in these domains is not at 42.5° to the plate boundary (the San

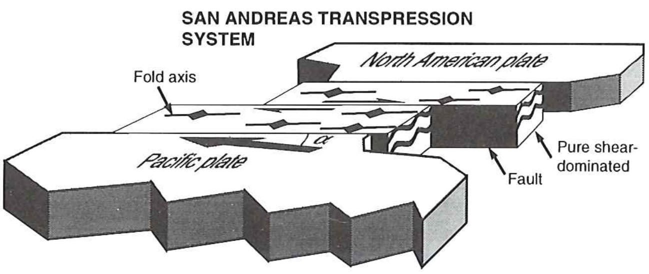

Fig. 13. Schematic illustration of the transpressional San Andreas fault system as viewed from the southwest. Pacific plate moves obliquely with respect to the American plate at an angle α of ca. 5°. Most of the simple shear component of the transpressional deformation along this plate boundary is accommodated by lateral shear along the faults, and the pure shear component of the total deformation therefore dominates the white blocks between the faults, causing folds with axes almost parallel to the faults.

Andreas fault), but lies at a much higher angle. Since the layering is sub-horizontal in the area, this provides a simple explanation as to why young fold axes in these domains generally make low angles (ca. 6–12°) with the fault system (Mount & Suppe 1987) (Fig. 13).

Results from our modeling may also be applied to the eroded, deep levels of ancient convergent plate boundaries or collision zones. For example, in the Caledonides, structures (lineations, fold axes, foliations, strains, etc.) vary considerably in different domains throughout the orogen. In the Norwegian Caledonides, the Møre–Trøndelag Fault Zone represents an anomalous zone of lateral shear deformation, at least during part of the Caledonian history, in an area of predominantly horizontal shortening and vertical thickening. Systematic fabric and strain analyses of this zone and surrounding units should be carried out with the contents of this article in mind, to test the hypothesis that the Caledonian deformation responded to oblique ($\alpha < 90°$), rather than perfectly orogen-perpendicular, collision.

Another possible example of strain partitioning was found in the adjacent Fosen area by Gilotti & Hull (1993), who explained the structural pattern in this area as due to partitioning into narrow sinistral strike-slip zones separating pure shear-dominated domains. Although it is generally hard to quantify this type of data from the hinterland in ancient convergent plate boundaries, the kinematics of these Caledonian systems indicate an oblique collision between Laurentia and Baltica so that the plate motion vector of the Laurentian plate had a more southerly direction relative to Baltica than the ESE direction usually inferred from lineations in the orogenic wedge (cf. Hossack & Cooper 1986).

Caledonian (Acadian) deformation in the Welsh Caledonides has also been shown to have a transpressive character (Soper & Hutton 1984). The strike-slip component of the sinistral transpression is here interpreted to have partitioned into steep strike-slip faults or into zones of steep bedding (Woodcock 1990). Although the orientation of the deformation zone is not very well defined, the low angle (ca. 7°) between what is interpreted as an incremental cleavage and hinge lines of early folds indicates that the deformation between the strike-slip faults is pure-shear dominated.

Strike-slip motion subparallel to the orogen also occurred after the Caledonian orogeny in Scandinavia, Scotland and Greenland. It has been argued that the convergent Caledonian plate motion was reversed and accompanied by severe extensional tectonics in early Devonian times (cf. Fossen & Rykkelid 1992). Extensional movement directions were more or less perpendicular to the length of the orogen (plate boundary) (Séranne & Séguret 1987; Fossen & Rykkelid 1992), but if orogen-parallel strike-slip movement accompanied the extension (e.g. Roberts 1983; Larsen & Bengaard 1991) we can conclude that on a large scale we are really looking at a partitioned transtensional rather than a pure extensional system. If some evidence (paleomagnetic or other) can be found for the amount of lateral movement, then this can be combined with estimates of the extension, and the flow apophyses, and thus the relative plate motion, can be reconstructed.

Conclusions

Strain modeling of transpression/transtension provides unique insight into three-dimensional deformation. Two classes of transpression and two classes of transtension (pure-shear dominated and wrench-dominated) are defined, based upon the relative magnitude of the instantaneous stretching axes. It has been demonstrated how the formation and evolution of geological structures (foliation, lineation, passive planar and linear markers) and the development of finite strain differ for the four different classes of transpression/transtension. Flow apophyses (axes of maximum gradient of the velocity field) define the movement of material points within transpressional/transtensional systems from centimeter to plate scale. The flow apophyses are the kinematic link between strain in the deformation zone and the boundary conditions. As a result, the flow apophyses give important information about the relative movement of rigid blocks on either side of a deformation zone, about the orientation of the shear zone boundaries in the system, and about the passive rotation of material lines and planes within the deformation zone. Therefore, this type of modeling allows predictions to be made about the structural implications of transpression/transtension which, when compared to natural systems, assists in tectonic analyses. Partitioning of the transpression (transtension) displacement field into broad domains dominated by contraction (extension) and separated by more discrete strike-slip shear zones or faults is ubiquitous in natural systems, particularly at plate boundaries. This situation can be accurately modeled using the general kinematic framework proposed here. The modeling of various degrees of partitioning, corresponding to different styles of deformation at various structural levels, allows us to analyze both neotectonic zones where brittle deformation dominates and exhumed deep levels of ancient orogens.

Acknowledgements. – This work was supported by a University of Minnesota doctoral dissertation fellowship for B.T. and grant EAR 9305262 from the National Science Foundation to C.T. Reidun Helming is thanked for help during computer programming. Reviews by A. G. Milnes and J. Gilotti helped improve the manuscript.

Manuscript received January 1994

References

Bell, T. H. 1981: Foliation development – the contribution, geometry and significance of progressive, bulk, inhomogeneous shortening. *Tectonophysics 75*, 273–296.

Bobyarchick, A. R. 1986: The eigenvalues of steady flow in Mohr space. *Tectonophysics 122*, 35–51.

Bürgman, R. 1991: Transpression along the southern San Andreas fault, Durmid Hill, California. *Tectonics 10*, 1152–1163.

Cashman, S. M., Kelsey, H. M., Erdman, C. F., Cutten, H. N. C. & Berryman, K. R. 1992: Strain partitioning between structural domains in the forearc of the Hikurangi subduction zone, New Zealand. *Tectonics 11*, 242–257.

DeMets, C., Gordon, R. G., Argus, D. F., & Stein, S. 1990: Current plate motions. *Geophysical Journal International 101*, 425–478.

Dennis, A. J. & Secor, D. T. 1990: On resolving shear direction in foliated rocks deformed by simple shear. *Geological Society of America Bulletin 102*, 1257–1267.

Diament, M., Harjono, H., Karta, K., Deplus, C., Dahrin, D., Zen, M. T., Gerard, M., Lassal, O., Martin, A. & Malod, J. 1992: Mentawai fault zone off Sumatra: A new key to the geodynamics of western Indonesia. *Geology 20*, 259–262.

Elliott, D. 1972: Deformation paths in structural geology. *Geological Society of America Bulletin 83*, 2621–2635.

Fitch, J. T. 1972: Plate convergence, transcurrent faults, and internal deformation adjacent to Southeast Asia and the Western Pacific. *Journal of Geophysical Research 77*, 4432–4460.

Fossen, H. & Rykkelid, E. 1992: Post-collisional extension of the Caledonide orogen in Scandinavia: structural expressions and tectonic significance. *Geology 20*, 737–740.

Fossen, H. & Tikoff, B. 1993: The deformation matrix for simultaneous simple shearing, pure shearing, and volume change, and its application to transpression/transtension tectonics. *Journal of Structural Geology 15*, 413–422.

Gilotti, J. A. & Hull, J. M. 1993: Kinematic stratification in the hinterland of the central Scandinavian Caldeonides. *Journal of Structural Geology 15*, 629–646.

Harding, T. P. 1985: Seismic characteristics and identification of negative flower structures, positive flower structures, and positive structural inversion. *American Association of Petroleum Geologists Bulletin 69*, 582–600.

Hossack, J. 1968: Pebble deformation and thrusting in the Bygdin area (Southern Norway). *Tectonophysics 5*, 315–339.

Hossack, J. R. & Cooper, M. A. 1986: Collision tectonics in the Scandinavian Caledonides. *In* Coward, M. P. & Ries, A. C. (eds.): Collision tectonics. *Geological Society of London Special Paper 19*, 287–304.

Hubbard, M. & Mancktelow, N. S. 1992: Lateral displacement during Neogene convergence in the western and central Alps. *Geology 20*, 943–946.

Hudleston, P. J., Schultz-Ela, D. & Southwick, D. L. 1988: Transpression in an Archaean greenstone belt, northen Minnesota. *Canadian Journal of Earth Sciences 25*, 1060–1068.

Jackson, J. 1992: Partitioning of strike-slip and convergent motion between Eurasia and Arabia in eastern Turkey and the Caucasus. *Journal of Geophysical Research 97*, 12471–12479.

Larsen, P.-H. & Bengaard, H.-J. 1991; Devonian basin initiation in East Greenland: a result of sinistral wrench faulting and extensional collapse. *Journal of the Geological Society of London 148*, 355–368.

Laubscher, H. P. 1971. The large scale kinematics of the western Alps and the northern Apennies and its palinspastic implications. *American Journal of Science 271*, 193–226.

Law, R. D., Knipe, R. J. & Dayan, H. 1984: Strain path partitioning within thrust sheets: Microstructural and petrofabric evidence from the Moine Thrust zone at Loch Eriboll, northwest Scotland. *Journal of Structural Geology 6*, 477–497.

Lister, G. S. & Williams, P. F. 1983: The partitioning of deformation in flowing rock masses. *Tectonophysics 92*, 1–33.

McCaffrey, R. 1991: Slip vectors and stretching of the Sumatran fore arc. *Geology 19*, 881–884.

McCoss, A. 1986: Simple constructions for deformation in transpression/transtension zones. *Journal of Structural Geology 8*, 715–718.

McKenzie, D. & Jackson, J. 1983: The relationship between strain rates, crustal thickening, paleomagnetism, finite strain and fault movements within a deforming zone. *Earth and Planetary Science Letters 65*, 182–202.

Means, W. D., Hobbs, B. E., Lister, B. E. & Williams, P. F. 1980: Vorticity and non-coaxiality in progressive deformations. *Journal of Structural Geology 2*, 371–378.

Mount, V. S. & Suppe, J. 1987: State of stress near the San Andreas Fault: implications for wrench tectonics. *Geology 15*, 1143–1146.

Mount, V. S. & Suppe, J. 1992: present-day stress orientations adjacent to active strike-slip faults: California and Sumatra. *Journal of Geophysical Research 97*, 995–12,013.

Oldow, J. S. 1990: Transpression, orogenic float, and lithospheric balance. *Geology 18*, 991–994.

Oldow, J. S., Bally, A. W., Ave Lallemant, H. G. & Leeman, W. P. 1989: Phanerozoic evolution of the North American Cordillera: United States and Canada. *In* Bally, A. W. & Palmer, A. R. (eds): The Geology of North America: an Overview. *Geological Society of America Bulletin*, 39–232.

Passchier, C. W. 1990: Reconstruction of deformation and flow parameters from deformed vein sets. *Tectonophysics 180*, 185–199.

Pinet, N. & Cobbold, P. R. 1992: Experimental insights into the partitioning of motion within zones of oblique subduction. *Tectonophysics 206*, 371–388.

Ramberg, H. 1975: Particle paths, displacement and progressive strain applicable to rocks. *Tectonophysics 28*, 1–37.

Ramsay, J. G. & Graham, R. H. 1970: Strain variation in shear belts. *Canadian Journal of Earth Sciences 7*, 786–813.

Ramsay, J. G. & Huber, M. I. 1983: *The Techniques of Modern Structural Geology: Strain Analysis*. Academic Press, London. 307 pp.

Ratschbacher, L. 1986: Kinematics of Austro-Alpine cover nappes: changing translation path due to transpression. *Tectonophysics 125*, 335–356.

Roberts, D. 1983: Devonian tectonic deformation in the Norwegian Calednoides and its regional perspectives. *Norges geologiske undersøkelse 380*, 85–96.

Sanderson, D. & Marchini, R. D. 1984: Transpression. *Journal of Structural Geology 6*, 449–458.

Séranne, M. & Séguret, M. 1987: The Devonian basins of western Norway: Tectonics and kinematics of an extending crust. *In* Coward, M. P., Dewey, J. F. & Hancock, P. L. (eds.): Continental extensional tectonics. *Geological Society of London Special Publication 28*, 537–548.

Simpson, C. 1983: Displacement and strain patterns from naturally occuring shear zone terminations. *Journal of Structural Geology 5*, 497–506.

Simpson, C. & De Paor, D. G. 1993: Strain and kinematic analysis in general shear zones. *Journal of Structural Geology 15*, 1–20.

Soper, N. J. & Hutton, D. H. W. 1984: Late Caledonian sinistral dispalcements in Britain: Implications for a three-plate collision model. *Tectonics 3*, 781–794.

Sylvester, A. G. 1988: Strike-slip faults. *Geological Society of America Bulletin 100*, 1666–1703.

Tapponnier, P., Peltzer, G. & Armijo, R. 1986: On the mechanics of the collision between India and Asia. *In* Coward, M. P. & Ries, A. C. (eds.): Collision Tectonics. *Geological Society Special Publication 19*, 115–157.

Tikoff, B. & Fossen, H. 1993: Simultaneous pure and simple shear: the unified deformation matrix. *Tectonophysics 217*, 267–283.

Tikoff, B. & Teyssier, C. T. 1994: Strain modeling of displacement-field partitioning in transpressional orogens. *Journal of Structural Geology 16*, 1575–1588.

Treagus, J. E. & Treagus, S. H. 1981: Folds and the strain ellipsoid: a general model. *Journal of Structural Geology 3*, 1–17.

Tron, V. & Brun, J.-P. 1991: Experiments on oblique rifting in brittle-ductile systems. *Tectonophysics 188*, 71–84.

Truesdell, C. 1953: Two measures of vorticity. *Journal of Rational Mechanical Analysis 2*, 173–217.

Vauchez, A. & Nicholas, A. 1991: Mountain building: Strike-parallel displacements and mantle anisotropy. *Tecontophysics 185*, 183–201.

Walcott, R. I. 1984: Geodetic strain and large earthquakes in the axial tectonic belt of North Island, New Zealand. *Journal of Geophysical Research 83*, 4419–4429.

Weijermars, R. 1991: The role of stress in ductile deformation. *Journal of Structural Geology 13*, 1061–1078.

Wilcox, R. E., Harding, T. P. & Seely, D. R. 1973: Basic wrench tectonics. *American Association of Petroleum Geologists Bulletin 57*, 74–96.

Withjack, M. O. & Jamison, W. R. 1986: Deformation produced by oblique rifting. *Tectonophysics 126*, 99–124.

Woodcock, N. H. 1986: The role of strike-slip fault systems at plate boundaries. *Philosophical Transactions of the Royal Society of London 147.*

Woodcock, N. H. 1990: Transpressive Acadian deformation across the Central Wales Lineament, *Journal of Structural Geology 12*, 329–337.

Zoback, M. D., Zoback, M. L., Mount, V. S., Suppe, J., Eaton, J. P., Healy, J. H., Oppenheimer, D., Reasenberg, P., Jones, L., Raleigh, C. B., Wong I. G., Scotti, O. & Wentworth, C. 1987: New evidence on the state of stress of the San Andreas fault system. *Science 238*, 1105–1111.

Zoback, M. D. & Zoback, M. L. 1991: Tectonic stress field of North American and Relative plate motions. *In* Engedahl, D. B., Zoback, M. D. & Blackwell, D. D. (eds.): *Tectonic Stress Field of North America and Relative Plate Motions*. Geological Society of America, Boulder, pp. 339–366.